The Journal of Immunology

Mechanisms of Oncostatin M-Induced Pulmonary Inflammation and Fibrosis

Afsaneh Mozaffarian, Avery W. Brewer, Esther S. Trueblood, Irina G. Luzina, Nevins W. Todd, Sergei P. Atamas and Heather A. Arnett

J Immunol 2008; 181:7243-7253; ;
doi: 10.4049/jimmunol.181.10.7243
http://www.jimmunol.org/content/181/10/7243

The Journal of Immunology is published twice each month by
The American Association of Immunologists, Inc.,
1451 Rockville Pike, Suite 650, Rockville, MD 20852

Print ISSN: 0022-1767 Online ISSN: 1550-6606.

Mechanisms of Oncostatin M-Induced Pulmonary Inflammation and Fibrosis

Afsaneh Mozaffarian,* Avery W. Brewer,† Esther S. Trueblood,† Irina G. Luzina,‡ Nevins W. Todd,‡ Sergei P. Atamas,‡ and Heather A. Arnett[1]*

Oncostatin M (OSM), an IL-6 family cytokine, has been implicated in a number of biological processes including the induction of inflammation and the modulation of extracellular matrix. In this study, we demonstrate that OSM is up-regulated in the bronchoalveolar lavage fluid of patients with idiopathic pulmonary fibrosis and scleroderma, and investigate the pathological consequences of excess OSM in the lungs. Delivery of OSM to the lungs of mice results in a significant recruitment of inflammatory cells, as well as a dose-dependent increase in collagen deposition in the lungs, with pathological correlates to characteristic human interstitial lung disease. To better understand the relationship between OSM-induced inflammation and OSM-induced fibrosis, we used genetically modified mice and show that the fibrotic response is largely independent of B and T lymphocytes, eosinophils, and mast cells. We further explored the mechanisms of OSM-induced inflammation and fibrosis using both protein and genomic array approaches, generating a "fibrotic footprint" for OSM that shows modulation of various matrix metalloproteinases, extracellular matrix components, and cytokines previously implicated in fibrosis. In particular, although the IL-4/IL-13 and TGF-β pathways have been shown to be important and intertwined of fibrosis, we show that OSM is capable of inducing lung fibrosis independently of these pathways. The demonstration that OSM is a potent mediator of lung inflammation and extracellular matrix accumulation, combined with the up-regulation observed in patients with pulmonary fibrosis, may provide a rationale for therapeutically targeting OSM in human disease. *The Journal of Immunology,* **2008, 181: 7243–7253.**

Oncostatin M (OSM)[2] is a cytokine in the IL-6 superfamily, a family characterized in part by the use of gp130 as a common receptor subunit (1, 2). Members of the family include IL-6, IL-11, LIF, G-CSF, ciliary neurotrophic factor, and cardiotrophin-1 (1, 2). Secreted primarily by T lymphocytes, macrophages, and neutrophils, OSM is known to be up-regulated in a variety of disease states that involve inflammation and has been implicated in diverse biological roles including bone formation, cartilage degradation, cholesterol uptake, pain, and inflammation (3–10). OSM signals through the use of the OSM receptor (OSMR) β subunit heterodimerized with gp130 (11). In humans, OSM can also signal through an additional receptor complex composed of LIF receptor coupled to gp130 (2). The OSMR/gp130 receptor complex is widely expressed on a variety of cell types, including epithelial cells, fibroblasts, chondrocytes, hepatocytes, and some neurons.

OSM has been demonstrated to be a potent modulator of extracellular matrix (ECM) in a variety of contexts, suggesting that OSM may be able to mediate seemingly opposite pathological consequences, including fibrosis (an excess of ECM) and cartilage degradation (a breakdown of ECM). Depending on tissue type and environmental milieu, both of these effects have been observed when OSM has been overexpressed or exogenously administered into lungs or joints of mice, respectively (12–14). In addition, OSM has previously been shown to be up-regulated in human pathologies where these types of consequences exist (3, 5, 7–9). Predominantly a locally acting cytokine, OSM is up-regulated in the synovial fluid from joints of patients with rheumatoid arthritis (RA) (3, 9), in the bronchoalveolar lavage (BAL) fluid of patients with scleroderma-associated interstitial lung disease (8), and in the livers of patients with cirrhosis (7). The proposed impact on ECM by OSM can be attributed in part to the ability of OSM to shift the balance between matrix metalloproteinases (MMP) and tissue inhibitors of metalloproteinase (TIMP). TIMPs bind to MMPs in a 1:1 ratio with a high affinity that results in a loss of MMP proteolytic activity. TIMP-1 and TIMP-3 have been previously shown to be differentially regulated by OSM, resulting in an increase in TIMP-1 and a decrease in TIMP-3 (15). In addition to regulating the digestion of ECM components, MMPs are also implicated in the cleaving and subsequent activation of a number of proteins, including TGF-β, a potent profibrotic cytokine (16). OSM has also been reported to be capable of directly inducing the transcription of type I collagen in vitro (17).

Fibrosis is a pathological hallmark of many of the human diseases associated with an elevation in OSM, and is characterized by an overproduction of ECM that is hypothesized to begin as a response to tissue damage or inflammation. Scleroderma, or systemic sclerosis (SSc), is an autoimmune disorder characterized by the fibrosis of skin and other organ systems in the presence of particular autoantibodies. Although SSc is a heterogeneous disease, the presence of lung fibrosis is a key prognostic indicator for patients and is the most common cause of death in this patient

*Department of Inflammation and †Department of Pathology, Amgen, Inc., Seattle, WA 98119; and ‡University of Maryland School of Medicine and Baltimore Veterans Affairs Medical Center, Baltimore, MD 21201

Received for publication April 24, 2008. Accepted for publication September 12, 2008.

The costs of publication of this article were defrayed in part by the payment of page charges. This article must therefore be hereby marked *advertisement* in accordance with 18 U.S.C. Section 1734 solely to indicate this fact.

[1] Address correspondence and reprint requests to Dr. Heather A. Arnett, Department of Inflammation, Amgen Corporation, 1201 Amgen Court West, Seattle, WA 98119. E-mail address: harnett@amgen.com

[2] Abbreviations used in this paper: OSM, oncostatin M; OSMR, OSM receptor; ECM, extracellular matrix; RA, rheumatoid arthritis; BAL, bronchoalveolar lavage; MMP, matrix metalloproteinase; TIMP, tissue inhibitors of metalloproteinase; SSc, systemic sclerosis; IPF, idiopathic pulmonary fibrosis; MSA, mouse serum albumin; TLDA, TaqMan Low Density Array; HRPT; hypoxanthine phosphoribosyltransferase; CTGF, connective tissue growth factor; OPG, osteoprotegerin.

Table I. *Characteristics of the volunteer groups*

Characteristic	Controls ($n = 6$)	SSc, No Alveolitis ($n = 7$)	SSc, Alveolitis ($n = 8$)	IPF ($n = 6$)
Age, mean ± SD, years	47.3 ± 14.3	49.4 ± 15.2	51.1 ± 12.7	55.3 ± 15.9
Sex, no. male/female	1/5	2/5	3/5	3/3
Race, no. Caucasian/African American	4/2	4/3	5/3	4/2
Total BAL protein, mean ± SD, μg/ml	64.6 ± 24.1	117.7 ± 31.6[a]	171.4 ± 79.9[a]	187.0 ± 84.7[a]

[a] Significant differences versus controls ($p < 0.05$) by unpaired two-tailed Student's t test for continuous variables or by χ^2 test for categorical variables.

population (18). We have previously demonstrated that OSM is up-regulated in the $CD8^+$ T cells in the lungs of scleroderma patients with interstitial lung disease, relative to those patients without lung disease or healthy controls (8).

In the current study, we demonstrate an up-regulation of OSM in the lungs of patients with not only scleroderma lung disease but also idiopathic pulmonary fibrosis (IPF). We also characterize the pathological consequences of having an excess of OSM in the lung, demonstrating a strong link between OSM and lung fibrosis.

Materials and Methods

Human BAL samples

The procedures for obtaining BAL samples from patients with IPF or scleroderma or from healthy volunteers were reviewed and approved by the University of Maryland Institutional Review Board. Characteristics of the volunteer groups are shown in Table I. Informed consent was obtained in all instances. The BAL procedures were as previously described (19). Six healthy volunteers underwent lavage procedures specifically for research purposes. BAL samples from patients with scleroderma lung disease were leftover samples from a previous study (19) stored at −80°C; none of the samples overlapped with the samples reported in Ref. 8. The presence or absence of alveolitis in patients with scleroderma was judged based on percentage of neutrophils or eosinophils ≥3 SD above the mean value for controls in differential BAL cell counts; the values of neutrophils ≥3.0% or eosinophils ≥2.2% of total cells were considered abnormally high (19). Seven BAL samples from SSc patients without alveolitis and eight BAL samples from SSc patients with alveolitis were used.

The BAL procedures are not commonly performed in IPF patients as part of their standard medical care because of the high risk/benefit ratio. Although bronchoscopy with BAL is occasionally performed to exclude infectious or neoplastic disease in these patients, such samples would be atypical by definition and not representative of the overall IPF baseline pathobiologic state. Although high-risk BAL in IPF patients may be performed for research purposes only, the goal of this study was not to correlate the OSM levels with disease severity or functional impairment, but rather to show the relevance of the findings to human disease. All six IPF patients in this study had end-stage lung disease and underwent lung transplantation due to the severity of their disease. The diagnosis of IPF was made based on history and physical examination, pulmonary function test data, radiographic findings, and lung pathology, according to the American Thoracic Society consensus statement on IPF (20). The IPF patients had median percent predicted values (first quartile, third quartile) of forced expiratory volume in one second of 40.5 (33.3, 56), forced vital capacity of 31 (30, 44), total lung capacity of 41 (37, 47.3), and diffusing capacity of the lung for carbon monoxide of 22.5 (16.8, 26.8). BAL was performed on explanted lungs from these IPF patients immediately following the explantation procedures in a manner that was technically similar to that done with bronchoscopy (19). In brief, the upper and lower lobe bronchi of the lung were identified. Using sterile technique, a 14 French Argyle Salem Sump tube (Tyco Healthcare/Kendall) was then wedged into a segmental bronchus in the upper lobe. A 150-ml volume of sterile saline was injected in 20-ml aliquots into the upper lobe and retrieved with manual syringe suction following each aliquot. Subsequently, a similar procedure was repeated for a segmental bronchus in the lower lobe. The lavage fluid from the upper lobe and lower lobe was placed in sterile containers and pooled for analyses. To validate this technique of BAL in the explanted lung, we were able to perform BAL procedures on two normal donor lungs, which were initially approved but ultimately not used for transplantation, as well as a BAL procedure on one explanted lung from a patient with scleroderma lung disease. Differential cell counts and total protein levels in the latter three samples were not different from those typically observed for the corresponding samples obtained by bronchoscopy (our unpublished results).

The fluid was delivered to the laboratory on ice. The samples were concentrated 10-fold using Macrosep centrifugal concentrators (Pall Filtron), and OSM concentration was measured using an ELISA kit from R&D Systems. Statistical analysis was performed using the two-sided Mann-Whitney U test, as compared with control. Total BAL protein was measured using a Bio-Rad protein assay kit.

Animals and reagents

Only female mice were used in all experiments. Six-to-eight-week-old BALB/c mice were obtained from Charles River Laboratories. Six-to-eight-week-old C57BL/6J mice were obtained from The Jackson Laboratory or from Taconic Farms. Ten-to-twelve-week-old C57BL/6 RAG2 knockout mice and C57BL/6 control mice were obtained from Taconic Farms. Eight-to-ten-week-old C57BL/6-KitW-v/J mast cell-deficient mice and littermate control mice were obtained from The Jackson Laboratory. Mice were acclimated for at least 1 wk, and experiments were performed with mice at the age of 8–12 wk. Five mice per group were used for all experiments, except three mice per group were used for the histological evaluations and the OSM time course experiment (see Fig. 2, *A–F*) and the early RNA expression profiling (see Fig. 5*C*). All animal procedures were conducted in complete compliance with the guidelines for the care and use of laboratory animals of the National Institutes of Health and were approved by the Institutional Animal Care and Use Committee of Amgen, Inc.

Mice were dosed by intranasal route with recombinant mouse OSM (R&D Systems) or mouse serum albumin (MSA; Sigma-Aldrich) control protein suspended in PBS and 0.1% BSA for up to 14 days. The proteins were administered in a 50-μl volume over both nares under isoflurane gas. In the IL-4, IL-13, and TGF-β cytokine blockade experiments, specific reagents and controls were obtained as follows: monoclonal anti-TGF-β1, -β2, -β3 (clone 1D11; R&D Systems), and mouse IgG1 control (clone 11711.11 or anti-AGP3-Pb; R&D Systems and Amgen in-house, respectively), anti-IL-4 receptor α-chain hybrid IgG1 mAb (Amgen in-house) and mouse IgG control (Sigma-Aldrich), IL-13 receptor α2 Fc (Amgen in-house), and human IgG control (Sigma-Aldrich). Endotoxin levels of all protein and Ab reagents were measured by the *Limulus* amebocyte lysate assay and were determined to be low endotoxin (endotoxin units <2 per mouse) for in vivo studies. At the termination of the study, mice were anesthetized using Avertin. Terminal bleeds were performed via the brachial artery before further manipulations. BAL fluid was collected in PBS as described further below. The right lung lobes were submerged in RNA-Later (Qiagen) and stored at −80°C for RNA isolation by minipreps (Qiagen, per manufacturer's protocol). The left lung lobe was snap frozen in liquid nitrogen and stored at −80°C for use in the Sircol collagen assay. For histological analysis, the entire lung was infused with formalin and embedded in paraffin for tissue preparations.

BAL fluid cell analysis and differentials

BAL was performed by intubating mice anesthetized with a 300-μl i.p. injection of 2.5% Avertin (2,2,2-tribromoethanol; Sigma-Aldrich) and flushing the lungs with two 600-μl volumes of PBS. BAL fluid was centrifuged at 100 relative centrifugal force for 7 min using an Eppendorf 5417C microcentrifuge. The BAL fluid supernatant was combined with PBS plus Tween 20 (Qbiogene) at a final concentration of 0.05% Tween 20 and frozen at −80°C for protein analysis. The cell pellet was gently resuspended with PBS containing 5% FBS (HyClone) for counting using a Siemens Advia 120 hematology machine (Bayer). A cytospin with ~15,000 cells was prepared using the Shandon Cytospin 3. Cells were

spun at 750 rpm for 6 min, then stained with Wright-Giemsa stain (Sigma-Aldrich) and allowed to air dry. A 100-cell manual differential was performed on each slide by light microscopy.

BAL fluid protein analysis

BAL fluid supernatants were used for activated mouse/rat/porcine/canine TGF-β1 protein expression analysis (R&D Systems Quantikine ELISA kit per manufacturer's recommendations). For the TGF-β1 ELISA, latent TGF-β1 in the BAL fluid was activated to the immunoreactive form by acid activation and base neutralization according to the R&D Systems protocol. Additional proteomic analysis of the BAL fluid samples (pooled from five mice per group) was performed by Rules-Based Medicine using their mouse MultiAnalyte Profile to measure 69 proteins in 240 μl of BAL fluid. A complete analyte list is available at www.rulesbasedmedicine.com.

Sircol collagen assay

The left lungs of mice were homogenized in a 15-ml conical tube containing 2 ml of 0.5 M acetic acid containing Complete protease inhibitor mixture (Roche Applied Science) and left on shaker overnight at 4°C. The following day tubes were centrifuged to separate debris, and supernatants were run over Qiashredder (Qiagen) columns two to three times. A total of 100 μl of supernatants (neat or diluted up to 4-fold) were used for the Sircol collagen assay per manufacturer's recommendations (Biocolor, distributed by Accurate Chemical). In brief, 1 ml of dye reagent was added to each sample and incubated on a shaker at room temperature for 30 min, then centrifuged at maximum speed for 10 min. Supernatants were removed from the pellet using low vacuum. The pellet was resuspended in 1 ml of alkali reagent, and 100 μl was transferred to a 96-well plate for absorbance reading at 540 nm. To quantify collagen in samples, a standard curve was produced using bovine type I collagen in 0.5 M acetic acid provided in the kit.

TaqMan Low Density Array (TLDA)

We created a custom TLDA card (Applied Biosystems) with inflammatory and fibrotic genes of interest and two housekeeping genes (18s RNA and mouse hypoxanthine phosphoribosyltransferase (HRPT)). cDNA was prepared using the High Capacity cDNA Archive kit (Applied Biosystems) using 1 μg of RNA. Assuming a 1:1 ratio of RNA:cDNA reverse transcription, 250 ng of cDNA in 250 μl was added to an equal volume of 2X TaqMan Universal PCR mix (Applied Biosystems). Approximately 50 ng or 100 μl was loaded onto four ports of the TLDA card and spun twice for 1 min at 1200 rpm in a Sorvall Legend. The card was sealed in a sealer (Applied Biosystems) and the injection ports were cut off and placed in the 7900HT Fast Real Time PCR System instrument (Applied Biosystems) using the SDS 2.2.2 software. Data analysis was performed using SDS 2.2.2 software using the "Relative Quant. (ΔΔCt) Study" assay (where "Ct" is threshold cycle), selecting the 384-well TLDA against HPRT as the endogenous control. ΔCts were copied into Excel and the log change relative to HPRT was calculated. Fold change for each gene was calculated by dividing the average relative expression to HPRT from mice in the OSM group by the average relative expression relative to HPRT from mice in the MSA group; $n = 3$ mice/group (early time point) or 5 mice/group (late time point). An asterisk indicates a p value <0.05 when comparing MSA vs OSM log expression relative to HPRT, for those genes with >2-fold difference.

Histopathology

For histopathological analysis, lungs were infused with 10% neutral buffered formalin and then placed in 10% neutral buffered formalin for 24 h. Lungs were then processed, embedded in paraffin, cut into 5-μm sections, and stained with H&E, periodic acid-Schiff, Masson's trichrome, and Picrosirius red for inflammation, mucin-secreting goblet cells, and fibrosis, using standard histological methods.

Statistical analysis

Differences in BAL OSM levels between human volunteers were evaluated using two-sided Mann-Whitney U test. To assess differences among groups of animals, statistical analyses were performed using Prism 4 software (GraphPad Software) using the unpaired t test. p values were considered significant if less than or equal to 0.05 ($p < 0.05$ denoted by ∗, $p < 0.01$ denoted by ∗∗, $p \leq 0.001$ denoted by ∗∗∗).

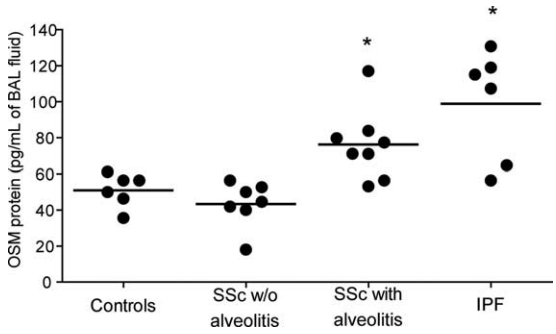

FIGURE 1. OSM is elevated in BAL fluids from patients with IPF and scleroderma patients with alveolitis compared with scleroderma patients without alveolitis or healthy controls. BAL fluid samples were harvested and analyzed for levels of human OSM by ELISA as described in *Materials and Methods*. Individual values are shown with means of each group represented with horizontal bars.

Results

OSM is elevated in human pulmonary fibrosis

The volunteer groups did not differ significantly in age, gender, or race (Table I). Consistent with the previous reports (21, 22) the levels of total BAL protein were increased in patients (Table I). ELISA of BAL fluids from healthy volunteers and scleroderma patients with or without interstitial lung disease confirmed previous findings (8) of an increase of OSM in the lungs of patients with scleroderma lung disease compared with scleroderma patients with no pulmonary involvement or with healthy controls (Fig. 1). Additionally, OSM levels were significantly increased in the lungs of patients with IPF (Fig. 1). These observations suggest that elevated pulmonary OSM levels may be associated with an ongoing fibrotic process rather than a specific disease. The increases of OSM in the scleroderma lung disease and IPF groups from the control group were statistically significant ($p = 0.033$ and $p = 0.045$, respectively, two-sided Mann-Whitney U test).

OSM administered to the lungs of mice results in an inflammatory and fibrotic response

To determine the pathological ramifications of excess OSM in the lungs of mice, recombinant mouse OSM was delivered daily by intranasal administration for up to 3 wk. Histological observation indicates that intranasal delivery of OSM in mice results in a diffuse subacute to chronic mononuclear and eosinophilic interstitial pneumonitis with fibrosis and contains some characteristics of IPF (Fig. 2). After 2 wk of daily treatment, the lungs of mice treated with OSM, compared with those receiving MSA as a control protein, had a significant inflammatory infiltrate as evidenced by H&E stain (Fig. 2*A*). The infiltrate was primarily composed of intraalveolar macrophages, eosinophils, giant cells, intraseptal infiltrates of macrophages, and lymphocytes (Fig. 2*E*). Similar infiltrates, also including plasma cells, were present around vessels and bronchioles (Fig. 2*E*). Lymphoid aggregates, interstitial fibrosis, and bronchiolar goblet cell hyperplasia were also present in H&E and periodic acid-Schiff-stained sections (Fig. 2*E*). Trichrome staining of the lung at 2 wk showed collagen deposition indicative of fibrosis (Fig. 2*D*). The collagen deposition appeared diffusely in the lung parenchyma, primarily within the alveolar walls in the lung and was accompanied with epithelial thickening and cellular infiltrates. Two different views from collagen-specific sirius red staining of the lung also showed a marked amount of mature, organized collagen deposition under bright light at 2 wk (Fig. 2*B*) and polarized light at 2 and 3 wk (Fig. 2*C*), confirming the results of the trichrome stain, as well as providing additional evidence of

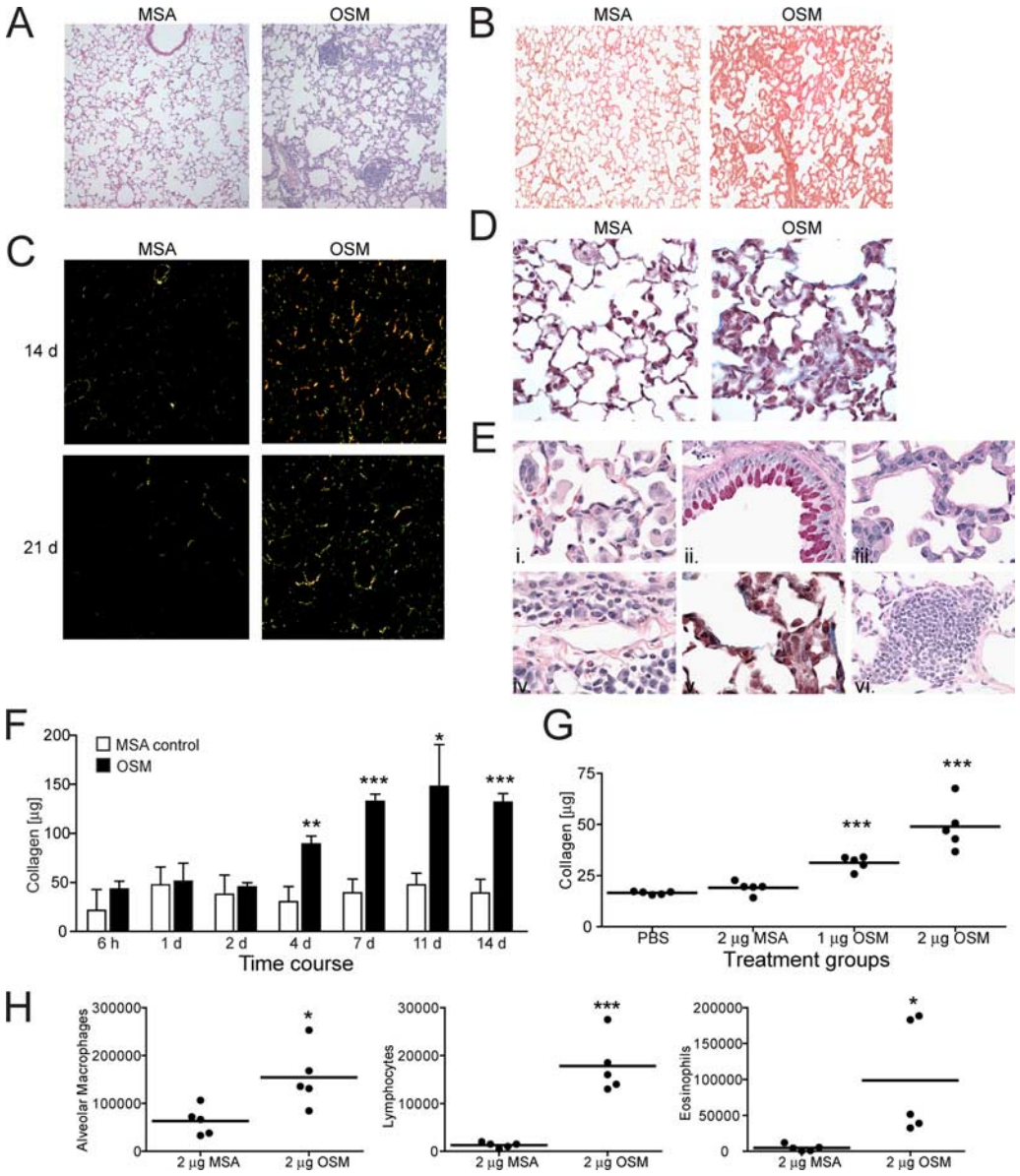

FIGURE 2. Local elevations in OSM result in lung inflammation and fibrosis in C57BL/6 mice. All of the histology data shown are representative of 2 wk, except where noted in *C*. *A*, H&E staining of the lungs of mice treated with 2 μg of OSM per day for 2 wk reveals a pronounced inflammatory infiltrate ($n = 3$ per group, $\times 10$). *B*, Picrosirius red staining is selective for new collagen, demonstrating an increase in new collagen formation in the lungs of mice treated with OSM for 2 wk ($\times 10$). *C*, Visualization of birefringent collagen using Picrosirius red under polarized light in mice treated daily with OSM for either 14 or 21 days ($\times 10$). *D*, Masson's trichrome histopathology shows an increase in collagen after 2 wk of treatment with OSM ($\times 40$, blue). *E*, Lung sections showing inflammatory infiltration (*i*), goblet cell hyperplasia (*ii*), and interstitial fibrosis (*iii–iv*), septal inflammation (*v*), and lymphoid aggregates (*vi*). *F*, Mice were treated daily with 2 μg of mouse OSM or a control protein (MSA) delivered intranasally. Lungs were harvested at the time points indicated (h = hours, d = days) and assayed for collagen levels by the Sircol assay ($n = 3$ per group). *G*, Lungs of five mice per group were collected after 11 days of treatment with either 1 or 2 μg of OSM daily and analyzed for collagen by Sircol assay. *H*, BAL fluid from five mice per group was collected after 11 days of OSM treatment with 2 μg of OSM and analyzed for cell differentials. An increase in the total number of alveolar macrophages, lymphocytes, and eosinophils was evident in OSM- vs MSA-treated groups. Each dot represents an individual mouse; $n = 5$ per group.

septal wall thickening. Lungs from mice dosed with intranasal OSM for 3 wk were examined by histology and exhibited similar results to mice dosed with intranasal OSM for 2 wk. There is no histopathological difference in fibrosis between mice treated for 2 or 3 wk, as measured by Masson's trichrome or Sirius red staining.

To quantify the amount of collagen deposition and to determine the time course of collagen accumulation, whole lungs were removed and analyzed for collagen using the Sircol assay. OSM induces a rapid accumulation of collagen, with a small but statistically significant increase in collagen observed by day 4. Collagen deposition continues to increase in a time-dependent manner until it levels off at day 7 and remains at a plateau at days 11 and 14 (Fig. 2*F*). The increase in collagen in response to OSM is dose dependent (Fig. 2*G*), and is similar in both C57BL/6 and BALB/c mice (data not shown). BALB/c mice are typically not considered to be prone to fibrosis; however, there are reports in the literature that show that various agents such as FITC induce lung fibrosis in the BALB/c mouse (23). Even the normally bleomycin "resistant" BALB/c mouse, can be significantly impacted by the addition of factors like cyclosporine A (24). Although we observed elevated collagen levels in BALB/c mice with OSM, we chose C57BL/6 mice for all of our future studies.

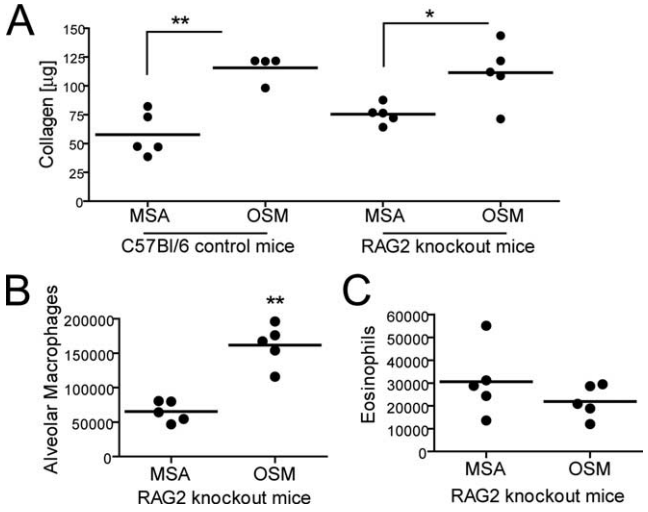

FIGURE 3. OSM-induced increases in collagen are independent of lymphocytes. RAG2 knockouts (on a C57BL/6 background) and control C57BL/6 mice were dosed daily with 2 μg of OSM or a control protein, MSA, for 11 days. Each dot represents an individual mouse; $n = 5$ per group. *A*, Lungs were harvested and assayed for total collagen content by the Sircol assay. No statistical difference in the collagen content of control mice and RAG2 knockouts following treatment with OSM is observed. *B* and *C*, Cell count differentials from the BAL fluid of RAG2 knockouts and control mice at day 11 are shown; recruitment of macrophages by OSM was intact in these mice. However, eosinophil recruitment was not observed in OSM-treated RAG2 knockouts.

To evaluate the accompanying inflammatory infiltrate, we collected BAL fluid from the lungs of C57BL/6 mice at the termination of the experiment and analyzed its cellularity. After 11 days, a significant recruitment of inflammatory cells is observed in the BAL fluid. The total number of white blood cells is increased in OSM-treated mice compared with MSA-treated controls, attributable to an increase in alveolar macrophages, eosinophils, and lymphocytes (Fig. 2*H*). Interestingly, although similar cellular infiltrate patterns and collagen deposition were observed in BALB/c mice, there was no eosinophilic infiltrate in response to OSM in this strain (data not shown).

Lymphocytes and mast cells are uninvolved in OSM-induced collagen changes

In our model of intranasal OSM-induced lung fibrosis, both inflammation and an increase in ECM are present. To determine whether these cellular infiltrates contribute to, or are required for, the fibrotic response to OSM, we used immune cell-deficient mice. Although OSM promotes an inflammatory infiltrate into the lungs, it was unknown whether the ECM in response to OSM is through direct interactions with the fibroblast and lung epithelial cells, or indirectly through the recruitment of inflammatory cells, which might express factors to contribute to fibrosis. Our data demonstrate a significant recruitment of lymphocytes into the BAL fluid of mice following intranasal OSM administration (Fig. 2*H*), and lymphocytes are known to produce a number of signals that can promote myofibroblast production and activation (25). Therefore, we obtained RAG2 knockout mice, lacking both B and T lymphocytes, and intranasally administered OSM or the control protein MSA daily for 11 days. Despite the lack of lymphocytes, RAG2 knockout mice treated with OSM displayed a similar increase in collagen deposition as that seen in control mice (Fig. 3*A*). Although the cellular composition of the BAL of RAG2 knockout mice contained an overall increase in total white blood cells, particularly in the macrophage subset (Fig. 3*B*), the increase was, predictably, much smaller when compared with control mice, due to the lack of lymphocytes in the RAG2 knockouts. We also observed a lack of eosinophil recruitment into the lungs in the RAG2 knockout mice (Fig. 3*C*). Combined with the similar disconnect between eosinophils and fibrosis in the BALB/c mice, this suggests that eosinophil infiltration to the lungs is likely not required for the collagen deposition induced by OSM. These observations are in agreement with previous work showing that T cells or eosinophils are not an absolute requirement for bleomycin-induced pulmonary fibrosis (26, 27).

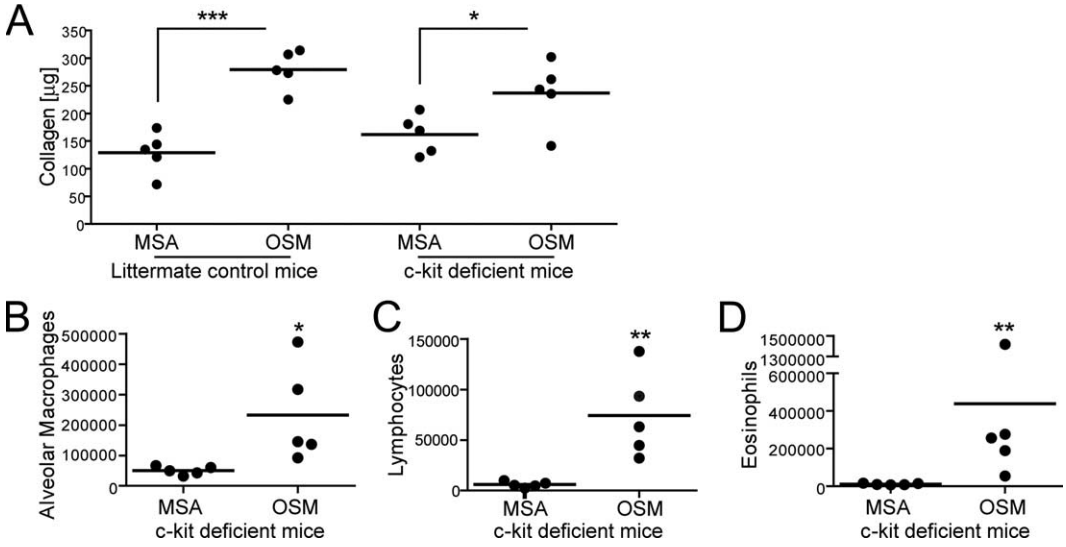

FIGURE 4. OSM-induced increases in collagen are independent of mast cells. Mast cell-deficient mice and littermate controls were dosed daily with 2 μg of OSM or a control protein, MSA, for 11 days. Each dot represents an individual mouse; $n = 5$ per group. *A*, Lungs were harvested and assayed for total collagen content by the Sircol assay. No statistical difference in the collagen content of control mice and mast cell-deficient mice following treatment with OSM is observed. *B–D*, Cell count differentials from the BAL fluid of mast cell-deficient mice and control mice at day 11 are shown; recruitment of macrophages, lymphocytes and eosinophils by OSM is intact in these mice.

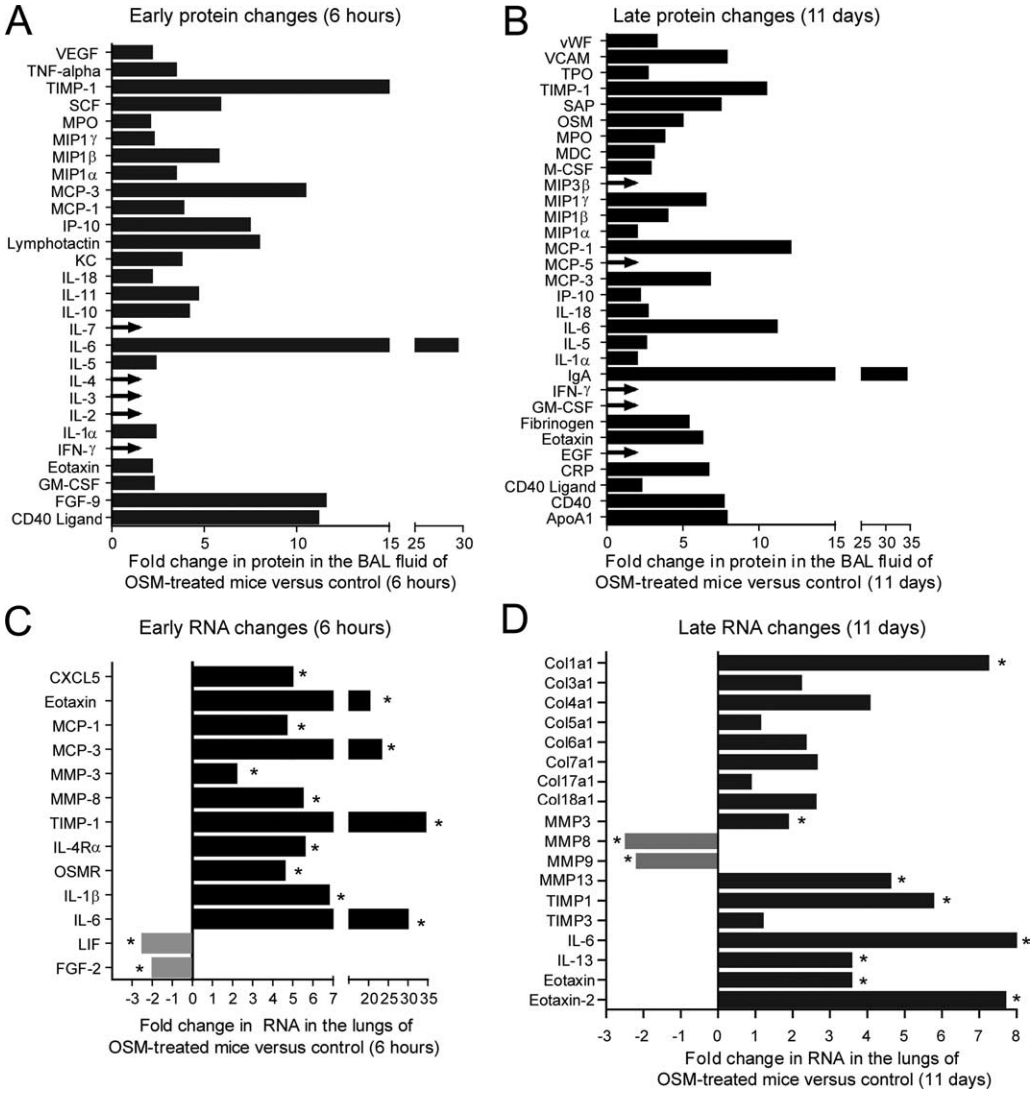

FIGURE 5. Changes in acute and chronic protein and gene expression following administration of OSM. *A*, C57BL/6 mice were treated with 5 μg of OSM, and BAL fluid was removed at 6 h postchallenge. Samples from five mice per group were pooled and analyzed for expression of 69 proteins using a multiplex-based multianalyte profiling. Proteins with fold changes of at least two times are shown. Arrows are used to represent an increase in cases where the MSA levels were below detection and OSM levels were high; therefore, fold change could not be calculated. *B*, C57BL/6 mice were treated with 2 μg of intranasal OSM daily for 11 days. BAL fluid was removed 11 days postchallenge. Samples from five mice per group were analyzed for expression of 69 proteins using a multiplex-based multianalyte profiling. Proteins with fold changes of at least two times are shown. Arrows are used to represent an increase in cases where the MSA levels were below detection and OSM levels were high; therefore fold change could not be calculated. *C*, Three C57BL/6 mice per group were treated with 2 μg of intranasal OSM or MSA control protein for 6 h. Lungs were individually processed for RNA analysis. Fold changes in gene expression were assessed by TLDA as described in *Materials and Methods*. Expression changes of at least 2-fold that were statistically significant ($p < 0.05$) are shown. *D*, Five C57BL/6 mice per group were treated daily for 11 days with 2 μg of OSM or MSA control protein, delivered intranasally, and lungs were individually processed for RNA analysis. Fold changes in gene expression were assessed by TLDA as described in *Materials and Methods*. Expression changes of at least 2-fold that were statistically significant ($p < 0.05$) as well as selected genes including collagens, MMPs, and TIMPs are shown.

In addition to eosinophils, we sought to further explore the role of other granule-storing immune cells, such as mast cells. We had observed that the ligand for c-*kit*, stem cell factor, was acutely up-regulated at the protein level by intranasal OSM (see Fig. 5*A*). Because c-*kit* ligand induces the proliferation of mast cells, and it has been previously reported that OSM can contribute to mast cell hyperplasia through a fibroblast-dependent manner (28), and mast cells have been reported to contribute to fibrosis (29, 30), we sought to determine whether mast cells may be involved in the fibrotic response observed with OSM by using mast cell-deficient mice. The inflammatory response and collagen deposition induced by OSM is intact in the mast cell-deficient mice (Fig. 4, *A–D*) suggesting mast cells are not required for either inflammation or fibrosis induced by OSM.

OSM induces an inflammatory and fibrotic footprint in the lungs

We have used both RNA from the lungs and protein from the BAL fluid of treated mice to elucidate a potential mechanism of action for OSM-induced inflammation and fibrosis. Multianalyte profiling of proteins and TLDA of a focused set of genes implicated in a fibrotic response were used to understand the acute inflammatory response caused by OSM as well as to analyze chronic remodeling changes.

Within 6 h of treatment with intranasal OSM, the BAL fluid contained a marked increase in a variety of proteins, particularly chemokines and cytokines (Fig. 5*A*). A wide array of chemokines,

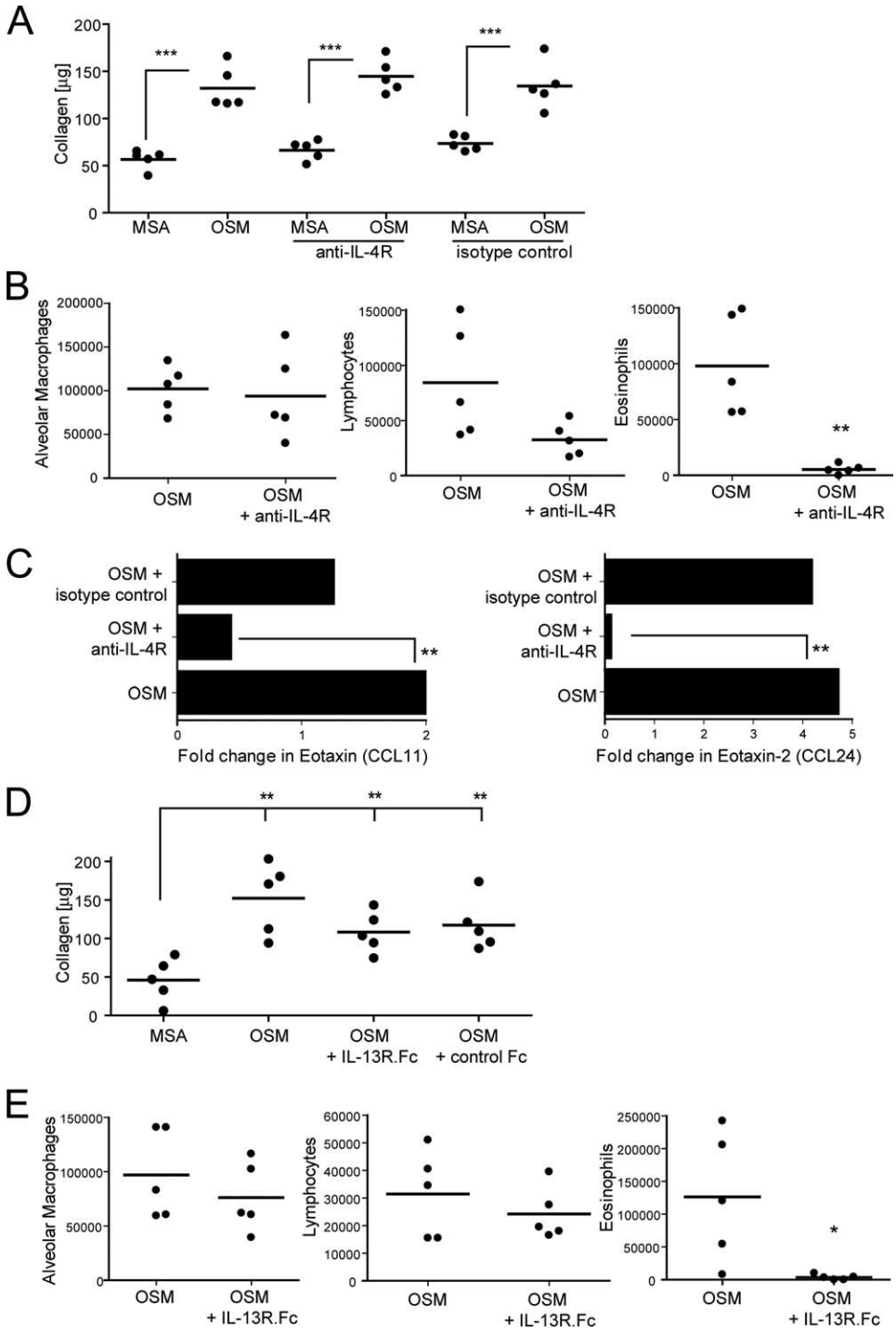

FIGURE 6. IL-4 and IL-13 are not required for the OSM-induced increase in collagen, but are required for eosinophil and lymphocyte recruitment. *A–C*, Five C57BL/6 mice per group were dosed i.p. with an Ab to IL-4R or an isotype control every other day for a total of six doses. *A*, Lungs were harvested and assayed for collagen content after 11 days. No changes were observed in the ability of OSM to induce new collagen formation following the blockade of the IL-4R. *B*, Cell-count differentials from the BAL fluid were performed at day 11; recruitment of eosinophils was not observed in the BAL fluid of mice with IL-4R inhibition. *C*, RNA from the lungs of five mice treated with OSM $^{+/-}$ anti-IL-4R were assayed for gene expression by TLDA. Eotaxin (CCL11) and eotaxin-2 (CCL24) expression are induced by OSM (Fig. 5*D*); however, this induction is blocked by an Ab to IL-4R. *D* and *E*, Five C57BL/6 mice per group were dosed i.p. with an Fc to IL-13R, along with appropriate control, every other day for a total of six doses. *D*, Lungs were harvested and assayed for collagen content after 11 days; OSM is still capable of inducing collagen formation in the absence of IL-13 signaling. *E*, Recruitment of eosinophils was not observed in the BAL fluid of mice with IL-13 inhibition on day 11. All data are representative of at least two separate experiments.

including eotaxin, MCP-1, MCP-3, MIP1α, MIP1β, and MIP1γ, were elevated in the BAL fluid, providing a likely mechanism for the rapid influx of inflammatory cells that occurs following OSM administration. In addition to chemokines, various cytokines were also up-regulated acutely in response to OSM, including IL-4, IL-1α, and IL-6. Similarly, at 11 days after daily intranasal OSM treatment, among all of the elevated analytes, many of the same chemokines and cytokines remained increased at high levels in comparison to the MSA controls (Fig. 5*B*).

To examine the gene changes that accompany the fibrotic response to OSM during acute and chronic administration, we assayed a variety of genes of interest by TLDA (Fig. 5, *C* and *D*). At the early time point of 6 h, OSM induced an increase in gene expression that included a variety of inflammatory cytokines and chemokines, such as IL-6, eotaxin, MCP-1, and MCP-3 (Fig. 5*C*) that mirrored the early protein findings in the BAL fluid (Fig. 5*A*). In contrast, chronic administration of OSM induced a different set of genes indicative of matrix remodeling (Fig. 5*D*). Confirming the histological findings, there was an elevation at the RNA level of several types of collagen following 11 days of administration of OSM, particularly type I collagen, the major structural component of ECM found in connective tissue and most internal organs. Various MMPs and TIMPs were differentially regulated, including increases in MMP-3 and MMP-13, decreases in MMP-8 and MMP-9, and an elevation in TIMP-1. Other increases in transcript levels in lungs of mice treated with OSM include IL-13 and the

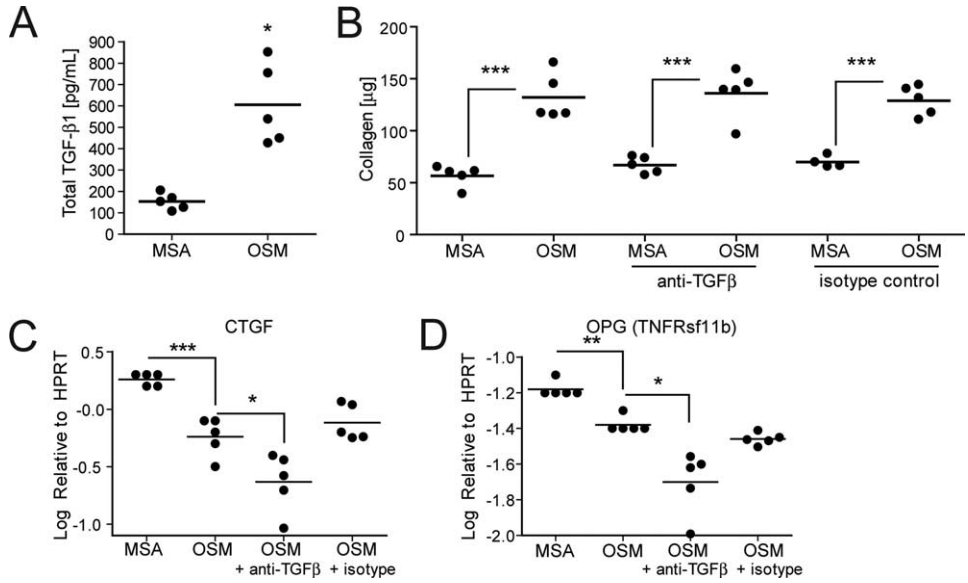

FIGURE 7. TGF-β is not required for the OSM-induced increase in collagen. *A*, BAL fluids were collected from C57BL/6 mice treated daily with 2 μg of OSM for 11 days, acid-activated, and assayed by ELISA for activated TGF-β1. Each dot represents an individual mouse; $n = 5$ per group. Active TGF-β1 was undetectable by ELISA in BAL fluids before acid activation (data not shown). *B*, Five C57BL/6 mice per group were dosed i.p. with an Ab to pan TGF-β1,2,3, or an isotype control Ab, every other day for a total of six doses. Lungs were harvested and assayed for collagen content after 11 days. No changes were observed in the ability of OSM to induce collagen deposition following the blockade of TGF-β. Data are representative of at least three separate experiments. *C* and *D*, RNA from the lungs of mice ($n = 5$ per group) treated with OSM$^{+/-}$ anti-TGF-β was assayed for changes in the gene expression of CTGF or OPG by TLDA; expression values are shown relative to a housekeeping gene, HPRT. CTGF and OPG expression are reduced with blockade of TGF-β.

eosinophilic chemokines eotaxin (CCL11) and eotaxin-2 (CCL24). Together, the protein and RNA data demonstrate early and late coordination of acute and chronic responses that contribute to the inflammatory and fibrotic response induced by OSM.

OSM-induced collagen deposition, but not eosinophil recruitment, is independent of IL-4/IL-13

Because IL-4 and IL-13 have been demonstrated to promote fibrosis under some circumstances, and we observed an increase in these analytes in mice treated with OSM, we hypothesized that OSM may be acting through this pathway to induce changes in ECM. We investigated their potential role using a blocking Ab to the IL-4 receptor, a receptor shared by both IL-4 and IL-13. In addition to signaling through the IL-4R, IL-13 has recently been proposed to be able to signal through a second receptor, IL-13Rα2; to ensure a complete blockade of IL-13 signaling, we also used an IL-13R.Fc that would block only IL-13 and not IL-4. In these experiments, lungs from mice that were treated every other day with 1 mg of IL-4R Ab or IL-13R.Fc exhibited an increase in collagen deposition with OSM that was similar to levels observed in the nontreated or isotype-treated controls (Fig. 6, *A* and *D*). These results suggest that although OSM induces both IL-4 and IL-13 (Fig. 5), the accumulation of collagen in the lungs induced by OSM is independent of both IL-4 and IL-13.

Interestingly, both the IL-4R Ab and the IL-13R.Fc completely blocked the eosinophil infiltrate induced by OSM (Fig. 6, *B* and *E*). In addition, although the message levels of eotaxin (CCL11) and eotaxin-2 (CCL24) were not altered by a control Ab (Fig. 6*C*) or anti-TGF-β (data not shown) treatment, both were markedly reduced to below baseline (Fig. 6*C*) by the anti-IL-4R Ab. Eotaxin and eotaxin-2 are eosinophilic chemokines, and their reduction in the presence of an IL-4R-blocking Ab is consistent with the prevention of eosinophil recruitment in response to OSM. The lack of eotaxin induction and eosinophil recruitment by OSM in these studies demonstrates their dependence on IL-13 and demonstrates that effective doses of the blocking reagents were achieved in vivo to block the relevant IL-4 and IL-13 pathways. This also confirms the previous finding from the RAG2 knockout study that eosinophil infiltration is not required for the OSM-induced ECM remodeling.

OSM-induced fibrotic changes are not dependent on TGF-β

TGF-β is perhaps the best studied of the profibrotic cytokines, and many profibrotic pathways ultimately operate through the activation of TGF-β. To define the role of TGF-β in OSM-induced lung fibrosis, we first wanted to determine whether TGF-β was present in the lungs of mice treated with OSM. Although OSM does not induce a change in the levels of TGF-β mRNA in the lungs of mice and we could not detect active TGF-β following OSM administration (data not shown), we observed an increase in acid-activated TGF-β1 by ELISA (Fig. 7*A*). These data indicate that TGF-β may be induced by OSM and present in latent form in the lung. To determine the dependence of OSM on TGF-β for the fibrotic response, mice were treated i.p. with either 100 or 250 μg of pan-anti-TGF-β 1,2,3 Ab (clone 1D11) or an isotype control, every other day, and challenged with 2 μg of intranasal OSM daily for 11 days. Mice treated with the anti-TGF-β Ab exhibited an increase in collagen deposition in response to OSM when compared with their MSA controls at levels comparable to the isotype treatment groups (Fig. 7*B*). Similar results were achieved with 100 μg of a soluble TGF-β receptor Fc reagent dosed every other day (data not shown). Administration of the Ab results in a decrease in the message level of connective tissue growth factor (CTGF) and osteoprotegerin (OPG), two genes previously shown to be downstream effectors of TGF-β function (Fig. 7, *C* and *D*) (16, 31). Modulation of both of these genes by the anti-TGF Ab, but not the isotype control (Fig. 7, *C* and *D*) or anti-IL-4R Ab (data not shown), suggests the doses of the Ab used were sufficient to impact

the target. Taken together, our results suggest that OSM represents a pathway that is sufficient to induce a fibrotic response independent of TGF-β.

Discussion

We have demonstrated that OSM, acting through the OSMR/gp130 heterodimer, is capable of producing a potent inflammatory and fibrotic response in vivo. Current treatments for fibrotic diseases such as scleroderma and IPF target the inflammatory cascade, but do not suppress the fibrotic process and show little efficacy in modulating the disease course. The expression of OSM in human disease and its ability to promote both inflammation and fibrosis in vivo may provide a rationale for therapeutically targeting OSM signaling in the context of fibrotic diseases.

We have shown that OSM is elevated in the lungs of patients with either scleroderma-associated interstitial lung disease or IPF (see Fig. 1), both inflammatory pulmonary diseases characterized by an accumulation of ECM. The purpose of these initial experiments was to demonstrate the relevance of OSM increase to human pulmonary pathology. Previous work has demonstrated that the presence of $CD8^+$ T cells from the BAL fluid of patients with SSc correlates with worse disease progression, and that the most highly changed gene relative to baseline in $CD8^+$ T cells is OSM (8). OSM has also been shown to be up-regulated in patients with liver cirrhosis, another condition involving the accumulation of excess ECM (7). Mice lacking the OSMR have delayed regeneration of the liver following surgical resection (32); fibrosis has been considered to be a wound-healing response gone awry (33), suggesting that the lack of a profibrotic cytokine may create a defect in wound healing. In addition to being found at high levels in human fibrotic diseases, OSM has also been shown to be up-regulated in the joints of patients with RA, an autoimmune disease resulting in cartilage degradation (3, 9). Although they are quite different types of pathology, fibrosis and RA are actually both inflammatory diseases involving a modulation of the ECM – either by its accumulation or by its degradation – and a fibroproliferative response is seen in the synovial tissue of RA patients. Our data and those of others show that OSM is a potent regulator of TIMP and MMP, suggesting one mechanism through which it may accomplish these seemingly polar roles.

In vitro, OSM has been demonstrated to promote fibroblast proliferation, predominantly through MAP kinase-dependent pathways (34–36). OSM can also inhibit fibroblast apoptosis (35), and may be able to promote epithelial-mesenchymal transition (EMT) to form myofibroblasts through activation of the JAK/STAT signaling pathways (37, 38). Fibroblastic foci are found to be overly abundant in patients with lung fibrosis and are thought to contribute to the pathogenesis of the disease and predict a worse prognosis in IPF (39, 40). In vivo, transgenic overexpression of bovine OSM under an islet cell promoter was demonstrated to cause a tissue-specific pancreatic inflammation and fibrosis, independent of its ability to induce IL-6 (41), and overexpression in the lung by virtue of an adenoviral system also caused a tissue-specific fibrotic response (13). The mechanism(s) of OSM-induced fibrosis could be multifold, but we have demonstrated that although the infiltration of inflammatory cells is a rapid response to OSM-stimulation of the lungs (likely due in part to the chemokine induction shown in Fig. 5*A*), the fibrotic response to OSM is largely independent of B cells, T cells, mast cells, and eosinophils – all cell types implicated in fibrotic responses under some conditions. Although both T cells and mast cells have been shown to express OSM in abundance in a variety of inflammatory situations, a recent review suggests that these cells are not always the drivers of pulmonary fibrosis and may only modulate the response (42).

TGF-β is a potent profibrotic cytokine, secreted primarily by inflammatory cells such as tissue macrophages, as well as circulating monocytes, fibroblasts, and epithelial cells. TGF-β is secreted in latent form and requires activation to exert its effects. After activation, TGF-β signaling occurs through transmembrane receptors that stimulate signaling intermediates, such as SMAD proteins to modulate transcription of procollagens I and III. This cytokine, primarily the TGF-β1 isoform, has been show to be a potent profibrotic stimulus in a variety of systems, and the results of its modulation in preclinical models have made it an attractive target for therapeutic manipulation in fibrotic diseases. However, conflicting data exist surrounding the TGF-β3 isoform that may suggest a regulatory role in fibrosis (43). Although TGF-β3 up-regulates SMAD proteins, it has been reported to down-regulate TGF-β1-induced gene expression, such as TIMP-1, collagen I, and CTGF, in some circumstances. However, it retains its ability to initiate profibrotic effects similar to those elicited by TGF-β1, albeit to a lesser degree. It's possible, however, that the current focus on inhibition of TGF-β and downstream SMAD may not be sufficient to prevent fibrosis due to a cooperative role between TGF-β and other profibrotic mediators that contribute to tissue remodeling. Although an anti-TGF-β1 Ab (Genzyme, CAT-192) did not meet its clinical endpoints in a recent phase I/II trial in patients with early diffuse SSc (44), further exploration of this pathway using pan-TGF-β inhibitors is necessary to rigorously test the hypothesis of its involvement in ongoing fibrosis.

Whereas the source of TGF-β tends to be mainly from innate immune cells, the source for another major profibrotic mediator, IL-13, is T_H2 $CD4^+$ T cells (33). IL-13 has been shown to contribute to fibrosis in a variety of models, including hepatic fibrosis induced by schistosome infection (45, 46) and lung fibrosis (47). IL-13 and other cytokines such as IL-4 and IL-5 have been previously demonstrated to also promote fibrosis, although the effects have been shown to come back, at least in part, to the induction of TGF-β. For instance, an IL-13 transgenic mouse overexpressing IL-13 in the lungs develops a pronounced fibrotic and inflammatory condition, and this can be largely reversed through inhibition of TGF-β with a soluble receptor Fc (47).

Because of the importance of TGF-β and IL-4/IL-13 pathways to fibrosis, and our data showing that IL-4 and IL-13 were up-regulated by OSM, we tested the dependence of OSM on TGF-β and IL-4/IL-13 using multiple approaches. A blocking Ab to IL-4R is effective in blocking the signaling actions of both IL-4 and IL-13 through the IL-4R/IL-13Rα1 heterodimer, as well as that of IL-4 signaling through the complex of IL-4R and the common γ-chain. IL-13 does also bind a second receptor with high affinity, IL-13Rα2 (48, 49). IL-13Rα2 appears to lack a signaling domain and has typically been demonstrated to act as a decoy receptor and capable of blocking the effects of IL-13 in vitro and in vivo (46, 50–53). However, two recent reports have implicated IL-13 signaling via IL-13Rα2 in the induction of TGF-β1, ultimately resulting in fibrosis (54, 55); therefore, we also used a mouse IL-13R.Fc, which would block all actions of IL-13 (but not IL-4). The use of these reagents allows us to conclude that the eosinophil recruitment by OSM is due to the induction of IL-13 and not IL-4, consistent with the published role of IL-13 in eosinophilic inflammation (56). However, these cytokines do not appear to be involved in the collagen deposition by OSM. We also tested the involvement of TGF-β using a previously characterized Ab and published dosing regimens, as well as a TGF-βR Fc, neither of which impacted the collagen accumulation induced by OSM. It is possible, due to the aforementioned potential regulatory effects of TGF-β3 in the fibrotic response, that the effects of blocking TGF-β1 and TGF-β2 were obscured by also blocking the TGF-β3

isoform. However, it has been shown that the protective role of TGF-β3 appears to be outbalanced by TGF-β1, and that the overexpression of TGF-β3 with TGF-β1 does not have any healing effects at early time points of the fibrotic response (14–28 days), during which our experiments were conducted.

In these studies, we have established a mechanistic basis for the induction of fibrosis by OSM, a cytokine capable of potent extracellular remodeling. By examining the ability of various cell types and cytokines to contribute to the pathology induced by OSM, we provide evidence for a novel profibrotic pathway that may be of therapeutic potential in human disease.

Acknowledgments

We thank Sam Tran and Michael Kuo for the analysis of the BAL fluid cell counts, Richard Smith for dosing animals on weekends, Penny Anders for assistance with tissue harvests, and Guang Chen for assistance with statistical analyses.

Disclosures

The authors have no financial conflict of interest.

References

1. Boulanger, M. J., and K. C. Garcia. 2004. Shared cytokine signaling receptors: structural insights from the gp130 system. *Adv. Protein Chem.* 68: 107–146.
2. Gearing, D. P., M. R. Comeau, D. J. Friend, S. D. Gimpel, C. J. Thut, J. McGourty, K. K. Brasher, J. A. King, S. Gillis, B. Mosley, et al. 1992. The IL-6 signal transducer, gp130: an oncostatin M receptor and affinity converter for the LIF receptor. *Science* 255: 1434–1437.
3. Cawston, T. E., V. A. Curry, C. A. Summers, I. M. Clark, G. P. Riley, P. F. Life, J. R. Spaull, M. B. Goldring, P. J. Koshy, A. D. Rowan, and W. D. Shingleton. 1998. The role of oncostatin M in animal and human connective tissue collagen turnover and its localization within the rheumatoid joint. *Arthritis Rheum.* 41: 1760–1771.
4. de Hooge, A. S., F. A. van de Loo, M. B. Bennink, D. S. de Jong, O. J. Arntz, E. Lubberts, C. D. Richards, and W. B. van den Berg. 2002. Adenoviral transfer of murine oncostatin M elicits periosteal bone apposition in knee joints of mice, despite synovial inflammation and up-regulated expression of interleukin-6 and receptor activator of nuclear factor-κB ligand. *Am. J. Pathol.* 160: 1733–1743.
5. Hasegawa, M., S. Sato, H. Ihn, and K. Takehara. 1999. Enhanced production of interleukin-6 (IL-6), oncostatin M and soluble IL-6 receptor by cultured peripheral blood mononuclear cells from patients with systemic sclerosis. *Rheumatology* 38: 612–617.
6. Kong, W., P. Abidi, F. B. Kraemer, J. D. Jiang, and J. Liu. 2005. In vivo activities of cytokine oncostatin M in the regulation of plasma lipid levels. *J. Lipid Res.* 46: 1163–1171.
7. Levy, M. T., M. Trojanowska, and A. Reuben. 2000. Oncostatin M: a cytokine upregulated in human cirrhosis, increases collagen production by human hepatic stellate cells. *J. Hepatol.* 32: 218–226.
8. Luzina, I. G., S. P. Atamas, R. Wise, F. M. Wigley, J. Choi, H. Q. Xiao, and B. White. 2003. Occurrence of an activated, profibrotic pattern of gene expression in lung $CD8^+$ T cells from scleroderma patients. *Arthritis Rheum.* 48: 2262–2274.
9. Manicourt, D. H., P. Poilvache, A. Van Egeren, J. P. Devogelaer, M. E. Lenz, and E. J. Thonar. 2000. Synovial fluid levels of tumor necrosis factor α and oncostatin M correlate with levels of markers of the degradation of crosslinked collagen and cartilage aggrecan in rheumatoid arthritis but not in osteoarthritis. *Arthritis Rheum.* 43: 281–288.
10. Morikawa, Y., S. Tamura, K. Minehata, P. J. Donovan, A. Miyajima, and E. Senba. 2004. Essential function of oncostatin m in nociceptive neurons of dorsal root ganglia. *J. Neurosci.* 24: 1941–1947.
11. Mosley, B., C. De Imus, D. Friend, N. Boiani, B. Thoma, L. S. Park, and D. Cosman. 1996. Dual oncostatin M (OSM) receptors: cloning and characterization of an alternative signaling subunit conferring OSM-specific receptor activation. *J. Biol. Chem.* 271: 32635–32643.
12. Hui, W., A. D. Rowan, C. D. Richards, and T. E. Cawston. 2003. Oncostatin M in combination with tumor necrosis factor α induces cartilage damage and matrix metalloproteinase expression in vitro and in vivo. *Arthritis Rheum.* 48: 3404–3418.
13. Richards, C. D., C. Kerr, L. Tong, and C. Langdon. 2002. Modulation of extracellular matrix using adenovirus vectors. *Biochem. Soc. Trans.* 30: 107–111.
14. Rowan, A. D., W. Hui, T. E. Cawston, and C. D. Richards. 2003. Adenoviral gene transfer of interleukin-1 in combination with oncostatin M induces significant joint damage in a murine model. *Am. J. Pathol.* 162: 1975–1984.
15. Gatsios, P., H. D. Haubeck, E. Van de Leur, W. Frisch, S. S. Apte, H. Greiling, P. C. Heinrich, and L. Graeve. 1996. Oncostatin M differentially regulates tissue inhibitors of metalloproteinases TIMP-1 and TIMP-3 gene expression in human synovial lining cells. *Eur. J. Biochem.* 241: 56–63.
16. Leask, A., and D. J. Abraham. 2004. TGF-β signaling and the fibrotic response. *FASEB J.* 18: 816–827.
17. Hasegawa, M., S. Sato, M. Fujimoto, H. Ihn, K. Kikuchi, and K. Takehara. 1998. Serum levels of interleukin 6 (IL-6), oncostatin M, soluble IL-6 receptor, and soluble gp130 in patients with systemic sclerosis. *J. Rheumatol.* 25: 308–313.
18. Steen, V. D., and T. A. Medsger. 2007. Changes in causes of death in systemic sclerosis, 1972–2002. *Ann. Rheum. Dis.* 66: 940–944.
19. Atamas, S. P., V. V. Yurovsky, R. Wise, F. M. Wigley, C. J. Goter Robinson, P. Henry, W. J. Alms, and B. White. 1999. Production of type 2 cytokines by $CD8^+$ lung cells is associated with greater decline in pulmonary function in patients with systemic sclerosis. *Arthritis Rheum.* 42: 1168–1178.
20. American Thoracic Society and European Respiratory Society. 2000. Idiopathic pulmonary fibrosis: diagnosis and treatment: international consensus statement. *Am. J. Respir. Crit. Care Med.* 161: 646–664.
21. Harrison, N. K., R. J. McAnulty, P. L. Haslam, C. M. Black, and G. J. Laurent. 1990. Evidence for protein oedema, neutrophil influx, and enhanced collagen production in lungs of patients with systemic sclerosis. *Thorax* 45: 606–610.
22. Phelps, D. S., T. M. Umstead, M. Mejia, G. Carrillo, A. Pardo, and M. Selman. 2004. Increased surfactant protein-A levels in patients with newly diagnosed idiopathic pulmonary fibrosis. *Chest* 125: 617–625.
23. Christensen, P. J., R. E. Goodman, L. Pastoriza, B. Moore, and G. B. Toews. 1999. Induction of lung fibrosis in the mouse by intratracheal instillation of fluorescein isothiocyanate is not T-cell-dependent. *Am. J. Pathol.* 155: 1773–1779.
24. Lossos, I. S., R. Or, V. Ginzburg, T. G. Christensen, Y. Mashriki, and R. Breuer. 2002. Cyclosporin A upmodulates bleomycin-induced pulmonary fibrosis in BALB/c mice. *Respiration* 69: 344–349.
25. Wynn, T. 2008. Cellular and molecular mechanisms of fibrosis. *J. Pathol.* 214: 199–210.
26. Hao, H., D. A. Cohen, C. D. Jennings, J. S. Bryson, and A. M. Kaplan. 2000. Bleomycin-induced pulmonary fibrosis is independent of eosinophils. *J. Leukocyte Biol.* 68: 515–521.
27. Helene, M., V. Lake-Bullock, J. Zhu, H. Hao, D. A. Cohen, and A. M. Kaplan. 1999. T cell independence of bleomycin-induced pulmonary fibrosis. *J. Leukocyte Biol.* 65: 187–195.
28. Gyotoku, E., E. Morita, Y. Kameyoshi, T. Hiragun, S. Yamamoto, and M. Hide. 2001. The IL-6 family cytokines, interleukin-6, interleukin-11, oncostatin M, and leukemia inhibitory factor, enhance mast cell growth through fibroblast-dependent pathway in mice. *Arch. Dermatol. Res.* 293: 508–514.
29. Navi, D., J. Saegusa, and F. T. Liu. 2007. Mast cells and immunological skin diseases. *Clin. Rev. Allergy Immunol.* 33: 144–155.
30. Oh, C. K. 2005. Mast cell mediators in airway remodeling. *Chem. Immunol. Allergy* 87: 85–100.
31. Thirunavukkarasu, K., R. R. Miles, D. L. Halladay, X. Yang, R. J. Galvin, S. Chandrasekhar, T. J. Martin, and J. E. Onyia. 2001. Stimulation of osteoprotegerin (OPG) gene expression by transforming growth factor-β (TGF-β): mapping of the OPG promoter region that mediates TGF-β effects. *J. Biol. Chem.* 276: 36241–36250.
32. Nakamura, K., H. Nonaka, H. Saito, M. Tanaka, and A. Miyajima. 2004. Hepatocyte proliferation and tissue remodeling is impaired after liver injury in oncostatin M receptor knockout mice. *Hepatology* 39: 635–644.
33. Wynn, T. A. 2004. Fibrotic disease and the T(H)1/T(H)2 paradigm. *Nat. Rev. Immunol.* 4: 583–594.
34. Ihn, H., and K. Tamaki. 2000. Oncostatin M stimulates the growth of dermal fibroblasts via a mitogen-activated protein kinase-dependent pathway. *J. Immunol.* 165: 2149–2155.
35. Scaffidi, A. K., S. E. Mutsaers, Y. P. Moodley, R. J. McAnulty, G. J. Laurent, P. J. Thompson, and D. A. Knight. 2002. Oncostatin M stimulates proliferation, induces collagen production and inhibits apoptosis of human lung fibroblasts. *Br. J. Pharmacol.* 136: 793–801.
36. Tong, L., D. Smyth, C. Kerr, J. Catterall, and C. D. Richards. 2004. Mitogen-activated protein kinases Erk1/2 and p38 are required for maximal regulation of TIMP-1 by oncostatin M in murine fibroblasts. *Cell. Signal.* 16: 1123–1132.
37. Nightingale, J., S. Patel, N. Suzuki, R. Buxton, K. I. Takagi, J. Suzuki, Y. Sumi, A. Imaizumi, R. M. Mason, and Z. Zhang. 2004. Oncostatin M, a cytokine released by activated mononuclear cells, induces epithelial cell-myofibroblast transdifferentiation via Jak/Stat pathway activation. *J. Am. Soc. Nephrol.* 15: 21–32.
38. Pollack, V., R. Sarkozi, Z. Banki, E. Feifel, S. Wehn, G. Gstraunthaler, H. Stoiber, G. Mayer, R. Montesano, F. Strutz, and H. Schramek. 2007. Oncostatin M-induced effects on EMT in human proximal tubular cells: differential role of ERK signaling. *Am. J. Physiol.* 293: F1714–F1726.
39. King, T. E., Jr., M. I. Schwarz, K. Brown, J. A. Tooze, T. V. Colby, J. A. Waldron, Jr., A. Flint, W. Thurlbeck, and R. M. Cherniack. 2001. Idiopathic pulmonary fibrosis: relationship between histopathologic features and mortality. *Am. J. Respir. Crit. Care Med.* 164: 1025–1032.
40. Willis, B. C., R. M. duBois, and Z. Borok. 2006. Epithelial origin of myofibroblasts during fibrosis in the lung. *Proc. Am. Thorac. Soc.* 3: 377–382.
41. Bamber, B., R. A. Reife, H. S. Haugen, and C. H. Clegg. 1998. Oncostatin M stimulates excessive extracellular matrix accumulation in a transgenic mouse model of connective tissue disease. *J. Mol. Med.* 76: 61–69.
42. Luzina, I. G., N. W. Todd, A. T. Iacono, and S. P. Atamas. 2008. Roles of T lymphocytes in pulmonary fibrosis. *J. Leukocyte Biol.* 83: 237–244.
43. Ask, K., P. Bonniaud, K. Maass, O. Eickelberg, P. J. Margetts, D. Warburton, J. Groffen, J. Gauldie, and M. Kolb. 2008. Progressive pulmonary fibrosis is mediated by TGF-β isoform 1 but not TGF-β3. *Int. J. Biochem. Cell Biol.* 40: 484–495.
44. Denton, C. P., P. A. Merkel, D. E. Furst, D. Khanna, P. Emery, V. M. Hsu, N. Silliman, J. Streisand, J. Powell, A. Akesson, et al. 2007. Recombinant human

anti-transforming growth factor β1 antibody therapy in systemic sclerosis: a multicenter, randomized, placebo-controlled phase I/II trial of CAT-192. *Arthritis Rheum.* 56: 323–333.
45. Chiaramonte, M. G., D. D. Donaldson, A. W. Cheever, and T. A. Wynn. 1999. An IL-13 inhibitor blocks the development of hepatic fibrosis during a T-helper type 2-dominated inflammatory response. *J. Clin. Invest.* 104: 777–785.
46. Chiaramonte, M. G., M. Mentink-Kane, B. A. Jacobson, A. W. Cheever, M. J. Whitters, M. E. Goad, A. Wong, M. Collins, D. D. Donaldson, M. J. Grusby, and T. A. Wynn. 2003. Regulation and function of the interleukin 13 receptor α 2 during a T helper cell type 2-dominant immune response. *J. Exp. Med.* 197: 687–701.
47. Lee, C. G., R. J. Homer, Z. Zhu, S. Lanone, X. Wang, V. Koteliansky, J. M. Shipley, P. Gotwals, P. Noble, Q. Chen, et al. 2001. Interleukin-13 induces tissue fibrosis by selectively stimulating and activating transforming growth factor β1. *J. Exp. Med.* 194: 809–821.
48. Donaldson, D. D., M. J. Whitters, L. J. Fitz, T. Y. Neben, H. Finnerty, S. L. Henderson, R. M. O'Hara, Jr., D. R. Beier, K. J. Turner, C. R. Wood, and M. Collins. 1998. The murine IL-13 receptor α 2: molecular cloning, characterization, and comparison with murine IL-13 receptor α 1. *J. Immunol.* 161: 2317–2324.
49. Zhang, J. G., D. J. Hilton, T. A. Willson, C. McFarlane, B. A. Roberts, R. L. Moritz, R. J. Simpson, W. S. Alexander, D. Metcalf, and N. A. Nicola. 1997. Identification, purification, and characterization of a soluble interleukin (IL)-13-binding protein: evidence that it is distinct from the cloned Il-13 receptor and Il-4 receptor α-chains. *J. Biol. Chem.* 272: 9474–9480.
50. Daines, M. O., and G. K. Hershey. 2002. A novel mechanism by which interferon-γ can regulate interleukin (IL)-13 responses: evidence for intracellular stores of IL-13 receptor α -2 and their rapid mobilization by interferon-γ. *J. Biol. Chem.* 277: 10387–10393.
51. Kawakami, K., J. Taguchi, T. Murata, and R. K. Puri. 2001. The interleukin-13 receptor alpha2 chain: an essential component for binding and internalization but not for interleukin-13-induced signal transduction through the STAT6 pathway. *Blood* 97: 2673–2679.
52. Wood, N., M. J. Whitters, B. A. Jacobson, J. Witek, J. P. Sypek, M. Kasaian, M. J. Eppihimer, M. Unger, T. Tanaka, S. J. Goldman, et al. 2003. Enhanced interleukin (IL)-13 responses in mice lacking IL-13 receptor α 2. *J. Exp. Med.* 197: 703–709.
53. Zheng, T., W. Liu, S. Y. Oh, Z. Zhu, B. Hu, R. J. Homer, L. Cohn, M. J. Grusby, and J. A. Elias. 2008. IL-13 receptor alpha2 selectively inhibits IL-13-induced responses in the murine lung. *J. Immunol.* 180: 522–529.
54. Fichtner-Feigl, S., I. J. Fuss, C. A. Young, T. Watanabe, E. K. Geissler, H. J. Schlitt, A. Kitani, and W. Strober. 2007. Induction of IL-13 triggers TGF-β1-dependent tissue fibrosis in chronic 2,4,6-trinitrobenzene sulfonic acid colitis. *J. Immunol.* 178: 5859–5870.
55. Fichtner-Feigl, S., W. Strober, K. Kawakami, R. K. Puri, and A. Kitani. 2006. IL-13 signaling through the IL-13alpha2 receptor is involved in induction of TGF-β1 production and fibrosis. *Nat. Med.* 12: 99–106.
56. Wynn, T. A. 2003. IL-13 effector functions. *Annu. Rev. Immunol.* 21: 425–456.